Photoelectric Properties of Oriented Bacteriorhodopsin/Polycation Multilayers by Electrostatic Layer-by-Layer Assembly

Jin-An He, Lynne Samuelson,† Lian Li, Jayant Kumar, and Sukant K. Tripathy*

Center for Advanced Materials, Departments of Chemistry and Physics, University of Massachusetts Lowell, Lowell, Massachusetts 01854

Received: March 24, 1998; In Final Form: June 3, 1998

Organized, heterogeneous polyelectrolyte assemblies using poly(dimethyldiallylammonium chloride) (PDAC) as the polycation and bacteriorhodopsin (bR) (purple membrane fragments, wild-type (WT-PM) and D96N mutant) as the polyanion have been successfully constructed using alternating electrostatic adsorption. The differential photocurrent of the PDAC/bR multilayer assemblies showed a light-on maximum photocurrent of 52 nA/cm^2 for PDAC/WT-PM (eight bilayers) and 80 nA/cm^2 for PDAC/D96N (six bilayers). These results indicate that the biological integrity and activity of bacteriorhodopsin are maintained after electrostatic deposition and that the photoelectric sensitivity of the D96N mutant is higher than that of the WT-PM. It was determined that the photocurrent in these assemblies increases with the adsorption of only the first few layers of bR and then declines with the increase in the number of bilayers. It was also found that the magnitude and polarity of the photocurrent are greatly dependent on the pH, which suggests that the current is strongly correlated with the local change of proton concentration at the electrode/electrolyte interface. Addition of sodium azide to the electrolyte was found to instantly increase the magnitude of the photocurrent of the WT-PM and then the photocurrent attached saturation when [NaN_3] > 100 mM, while an initial increase and then a decrease of the photocurrent was observed with the D96N mutant. These results show that the differential photocurrent of bR results originally from the action of formation and decay of the M intermediate, which then leads to the local change of proton concentration at the electrode/electrolyte interface. That is, the formation of M intermediate (which results in an increase of proton concentration at the electrode/electrolyte interface due to proton release of bR) produces the light-on photocurrent, while the decay of M intermediate (which results in a decrease of proton concentration at the interface due to proton uptake of bR) contributes to the light-off photocurrent.

1. Introduction

Bacteriorhodopsin (bR) is a protein−chromophore complex that serves as a light-driven proton pump in the purple membrane (PM) of *Halobacterium salinarium.*[1] The retinal chromophore, which contributes the purple color of PM, is covalently attached to the polypeptide chain of bR at lysine-216 via a protonated Schiff base. Under illumination by yellow light, bR undergoes a photochemical cycle which pumps protons across the membrane from the inside of the cell to the outer medium. The resulting proton gradient generates electrochemical energy which is used by *H. salinarium* to synthesize ATP from inorganic phosphate and ADP.[2,3]

The X-ray structure of bR with 2.5 Å resolution has been recently reported by Pebay-Peyroula and co-workers.[4] From this detailed structure, the trajectory of the transported proton is defined by the Schiff base, at least eight water molecules, and several amino residues (Asp85, Asp96, Arg82). When the retinal is isomerized from all-trans to 13-cis by a photon, the Schiff base donates a proton to the anionic Asp85, and the M intermediate is formed. Subsequently, the proton is released into the extracellular solution via the pathway formed by water molecules, Arg82 and Thr205. When the M state decays, the Schiff base is reprotonated from Asp96, which subsequently takes up a proton from the cytoplasmic solution.[5−7] The sequence of proton release before proton uptake occurs at neutral and high pH. At low pH (pH < 5), proton uptake can occur before release.[8,9]

Long-term stability against thermal, chemical, and photochemical degradation together with desirable photoelectric and photochromic properties has made bR one of the most promising biological candidates for the bioelectronics field. For example, an imaging device[10] and a light-sensitive alarm device[11] have been constructed based on the differential photocurrent of PM which is in the millisecond time range. There are, however, conflicting opinions regarding the actual molecular mechanism of the differential photocurrent. Miyasaka and co-workers have suggested that the charge displacement within the bR induces a current on the electrode adjacent to the bR molecule when bR is excited by light.[12] Robertson and Lukashev, however, have reported that the differential current of bR results from an electrochemical current induced by the local pH change and not by charge displacement.[13] More recently, studies from El-Sayed and co-workers support this latter conclusion. In their work, comparative studies were carried out under pulsed and CW laser photoexcitations on different time scales (from nanoseconds to milliseconds); a correlation was found between the slow B3 photocurrent component under pulsed laser excitation and the D1 differential current component from CW laser excitation. Since the B3 component results from the proton

† Science and Technology Directorate, U.S. Army Natick Research, Development and Engineering Center, Natick, MA 01760.

* To whom correspondence should be addressed.

S1089-5647(98)01612-5 CCC: $15.00
Published on Web 08/13/1998

accumulation near the electrode/bR interface, the origin of the D1 photocurrent should be the same as for B3. In general, the photocurrents of both B3 and D1 result from the change of proton concentration at the electrode/electrolyte interface as a result of the proton pumping of bR, which leads to the formation of a transient proton capacitor between the working and counter electrodes. The charging and discharging processes of the proton capacitor produce the differential photoelectric response of bR.[14]

A simple technique of ultrathin film assembly has been developed which uses the alternate layer-by-layer electrostatic deposition of oppositely charged polyelectrolytes.[15] We have recently applied this approach to the deposition of bR[16] where it was determined that oriented PM layers are formed which give reasonably high second-order susceptibilities: $\chi^{(2)}$ of 8.1×10^{-9} esu which is larger than the maximum value of 5.4×10^{-9} esu reported so far, obtained from films prepared by the electrical sedimentation method.[17] The better the orientation and acentric order of PM in the films, the larger the nonlinear optical coefficient obtained. This result indicates that the degree of acentric order of bR in the PDAC/bR films is as good as, if not better than, that obtained in electric-field-oriented bR films. In this paper, the differential photoelectric response of the electrostatically deposited PDAC/bR assemblies is investigated under various pH and NaN_3 concentrations of the electrolyte. The results show that the electrostatic layer-by-layer technique is a simple, versatile, and useful method for the preparation of ordered, photoactive bR films. In addition, the effect of NaN_3 and pH on the photocurrent supports the conclusion that the differential photocurrent of bR results from the local pH change which is due to proton pumping of bR and that it is the formation and decay of the M intermediate in the bR photocycle that causes the local change of proton concentration at the electrode/electrolyte interface.

2. Materials and Methods

Bacteriorhodopsin (wild type, WT) in the form of the purple membrane (PM) was isolated from *Halobacterium salinarium* strain R_1M_1 according to a standard method described previously.[18] The purity was confirmed using the absorption ratio of $A_{280\ nm}/A_{570\ nm}$. This ratio was 2.0 for our sample, which indicated a good quality sample.[19] The D96N mutant, whose protonable aspartate at the 96 position is exchanged by a nonprotonable asparagine, was obtained from Dr. Howard H. Weetall at the National Institute of Standards and Technology (NIST, Gaithersburg, MD). The stock solutions of the WT-PM and D96N were stored at 4 °C in Milli-Q water before use. Poly(dimethyldiallylammonium chloride) (PDAC, medium molecular weight, 20 wt % in water) was purchased from Aldrich Chemical Co. and used as the polycation without further purification. In the electrostatic adsorption experiments the bR suspensions were used at a concentration of 0.5 mg/mL (wild type or D96N mutant, 1.2 OD at 570 nm calculated according to $\epsilon = 63\,000\ M^{-1}\ cm^{-1}$ and MW = 26 000),[20] and the pH was adjusted to 9.4 using 0.1 M NaOH aqueous solutions before every experiment. PDAC was dissolved in Milli-Q water at a concentration of 2.0 mg/mL containing 0.5 M NaCl and at a pH of 6.8 for the multilayer adsorption.

A detailed description of the electrostatic deposition of the bR assemblies is given in a previous publication.[16] In brief, the surface of a solid support (glass or indium tin oxide (ITO)) is pretreated to render a net negative surface charge by placing it in a 2% KOH aqueous solution under sonication and heating at 25 °C for 30 min. The support is then immersed in the polycationic, PDAC solution, for 5 min, rinsed in Milli-Q water for 2 min, and then dried with nitrogen. The layered support is then transferred into a 0.5 mg/mL bR suspension (pH 9.4) for 5 min, rinsed with water (pH 9.4) for 2 min, and dried by nitrogen. This process is repeated until the desired number of bilayers of PDAC/bR is obtained. All adsorption procedures were carried out at room temperature.

The photoelectric properties of the PDAC/PM films were studied using a setup consisting of a halogen lamp (50 W), a combined long-pass filter and heat-absorbing filter which provided yellow light from 530 to 750 nm with 10 mW/cm^2 incident power, an electric shutter, an optical glass electrochemical cell ($50 \times 50 \times 50$ mm), an autoranging picoammeter (Keithley 485), and a digitizing oscilloscope (HP 54510B, 300 MHz) with an IEEE 488 interface connected to a microcomputer for data acquisition. The 6 ms rise time of the picoammeter (200 nA range) is the response time of the system. The ITO conductive glass electrode ($35 \times 12 \times 1$ mm) deposited with PDAC/bR multilayers was used as the working electrode, and the counter electrode was a platinum wire 1.0 mm in diameter. The distance between the two electrodes in the electrochemical cell was 1.5 cm, and the cell was connected so that the positive current represented the direction that positive charge moved from the working electrode via the current meter to the Pt electrode. All photocurrent measurements were conducted in air at room temperature, with 80 mL of 0.5 M KCl aqueous solution as the supporting electrolyte. The pH of the supporting electrolyte solution was adjusted with 0.1 M KOH or HCl. To minimize the signal-to-noise ratio, the photoelectric signal was averaged from 5 to 10 times by the digitizing oscilloscope. UV−vis absorption spectra were recorded using a Perkin-Elmer Lambda-9 UV/vis/near-IR spectrophotometer. Milli-Q water was used for all electrostatic deposition and photoelectric studies. Other chemicals (NaCl, KCl, HCl, KOH, and NaOH) were ACS reagents from Aldrich and were used as received.

3. Results and Discussion

3.1. Structure of the PDAC/bR Multilayers. Bacteriorhodopsin is known to have a very high negative surface charge density of approximately two negative charges per bR molecule.[21] Moreover, the charge density is known to change with pH and ionic strength of the solution.[22,23] Therefore, it is feasible that under the proper conditions bR may be electrostatically layered using a suitable polycation as the alternating counterion layer. In this way multilayer assemblies composed of alternating layers of the polycation, PDAC, and the polyanion, bR, were prepared. Figure 1 shows the UV−vis absorption spectra for the sequential deposition of PDAC/bR bilayers (Figure 1a for WT-PM and Figure 1b for D96N mutant) at each consecutive step of the multilayer assembly process. From the figure it can be seen that the multilayer growth of the PDAC/bR assemblies is linear and reproducible. The characteristic absorption peaks for bR at 278 and 563 nm are observed to increase proportionately with each additional bilayer as shown in the inset of Figure 1.

In our previous work, characterization of the orientation and degree of order of the PDAC/WT-PM assemblies was carried out using ellipsometry, second harmonic generation, and atomic force microscopy.[16] These results confirmed that organized monolayers of WT-PM are, in fact, obtained within the PDAC/PM bilayers and that the final thickness of the PDAC/WT-PM assemblies may be controlled by simply repeating the layer-by-layer adsorption as desired. Figure 2 is a schematic of the configuration of the polyion and the purple membrane fragment

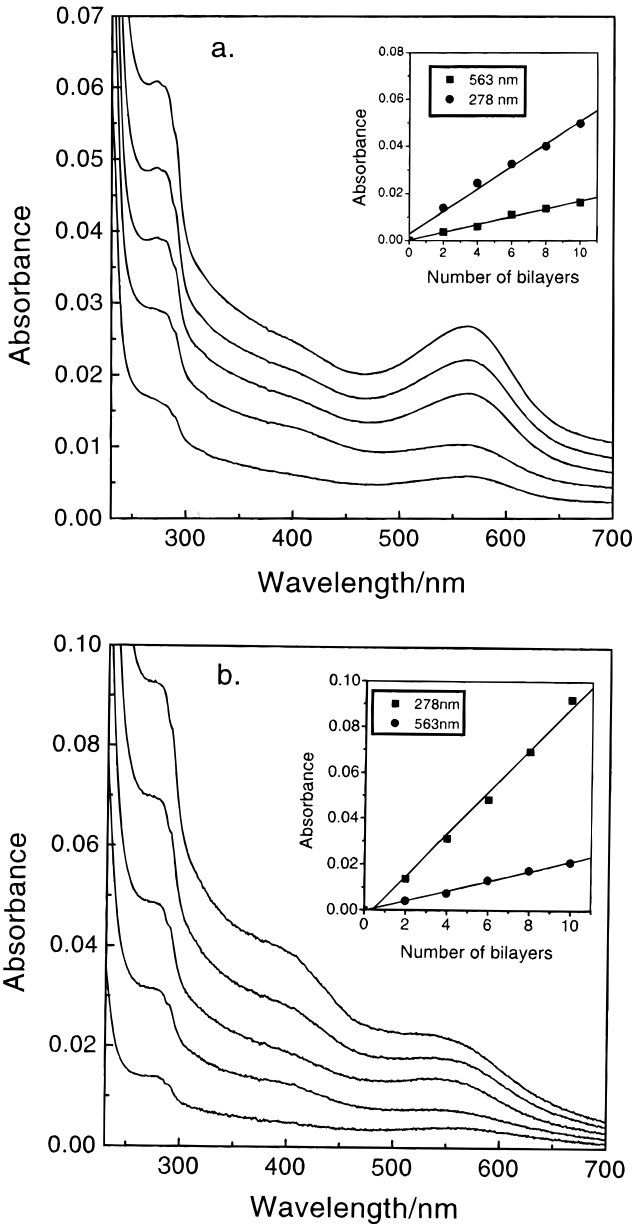

Figure 1. UV−vis absorption spectra of PDAC/bR multilayers (a) for WT-PM and (b) for D96N mutant on a quartz slide. The curves, from bottom to top, correspond to adsorption of 2, 4, 6, 8, and 10 alternate PDAC/bR bilayers, respectively. The inset shows the increase of absorbance at 278 and 563 nm with the number of bilayers. The baseline increase is due to light scattering from the multilayers, and its contribution has been deducted from the total absorbance.

in these assemblies. As shown, a monolayer of the polycation, PDAC, is first electrostatically adsorbed onto the pretreated negatively charged surface of the solid support, and then a monolayer of the polyanion, bR, is electrostatically adsorbed onto the PDAC layer. Since the cytoplasmic side of bR is known to contain more negative charges than the extracellular side under alkline condition,[21,23] it is believed that the cytoplasmic side of the bR predominantly attaches to the PDAC layers in these assemblies in the electrostatic adsorption process.

This layer-by-layer electrostatic deposition technique offers several advantages for the preparation of organized thin films of bR over previously established techniques such as the Langmuir−Blodgett (LB) method,[24] electrical sedimentation,[25] and antigen−antibody recognition.[26] One major advantage is that the method is extremely facile where no specialized equipment, modified chemicals, and time-consuming preparation

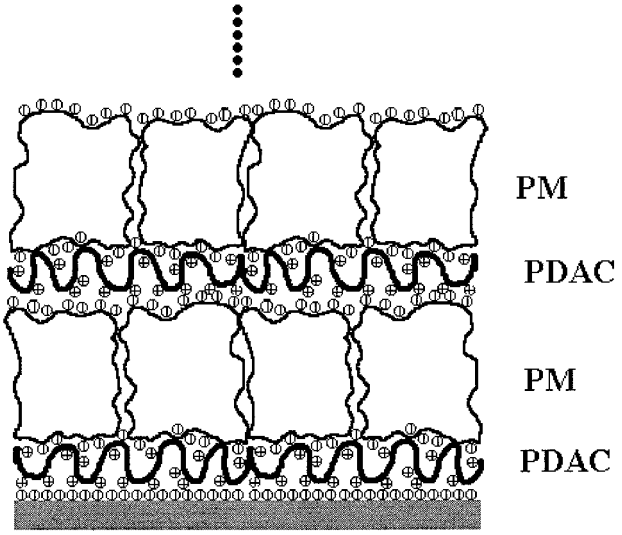

Figure 2. Schematic illustration of PDAC/bR multilayers.

procedures are required. This process, which can be carried out on a benchtop, requires only the preparation of two simple solutions, a few beakers, and approximately 15 min time to deposit an organized PDAC/bR bilayer. Another advantage is the versatility of this technique to integrate bR with other interesting systems. Since this approach has already been successfully applied to a variety of charged molecules such as conducting polymers,[27] nanoparticles,[28] proteins,[29] and ceramics,[30] it is reasonable to believe that these types of molecules could also be easily intercalated with the bR to either enhance the bR properties or add additional functionality to the final assemblies for a host of potential bioelectronic applications.

3.2. Photoelectric Response of PDAC/PM Multilayers. The photosensitive differential photocurrent from bR is an important and desirable property for bioelectronic device applications. Moreover, the magnitude and efficiency of the differential photocurrents that can be generated from bR films is quite dependent on the effectiveness of a bR layering technique. The typical photoelectric responses for eight bilayers of PDAC/WT-PM ((PDAC/WT-PM)$_8$) and six bilayers of PDAC/D96N ((PDAC/D96N)$_6$) are given in Figure 3, a and b, respectively. The positive peak photocurrent (light-on photocurrent) is relative to turning the light on, and the negative peak (light-off photocurrent) corresponds to turning the light off. The insets in each figure show the dependence of the magnitude of the light-on photocurrents on the pH of the electrolyte solution. It is observed that the WT-PM and D96N mutant generate substantial differential currents which indicates that the physiological activity of the bR in both of these systems is preserved after electrostatic deposition. The time scale and magnitude of the these photoelectric observations show some differences in comparison with previous reports,[12−14] which may be explained by variables such as bR concentration, film thickness, light intensity and irradiation area, electrolyte composition, and the type of electrode.[31] However, the differential response properties of these currents, including their dependence on pH of the electrolyte solution,[13,32] are in excellent agreement with those previously obtained using other layering techniques.

It is also important to note that the ratio of the magnitude of the light-on/light-off photocurrent from the WT-PM assembly (approximately 1.2) is much smaller than that observed for the D96N mutant (approximately 2.8). Also, the time scale (defined from maximum peak current to zero) of the WT-PM (about 500 ms for both light-on and light-off currents) is significantly

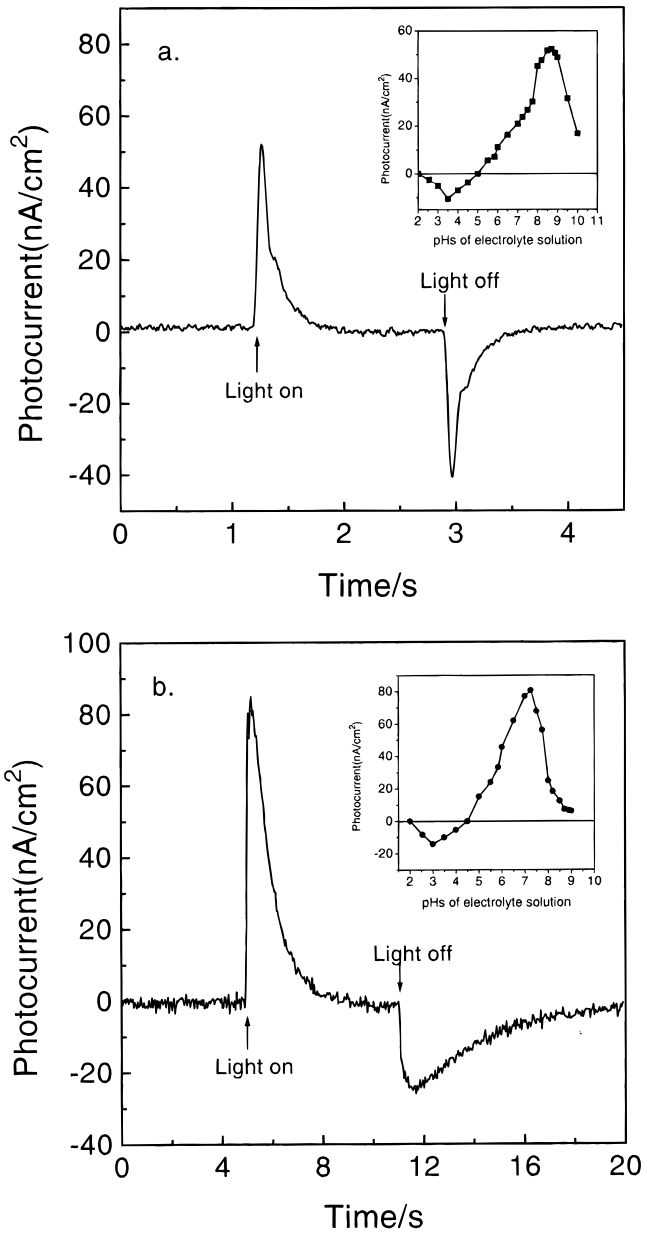

Figure 3. Differential photocurrent from (a) $(PDAC/WT\text{-}PM)_8$ and (b) $(PDAC/D96N)_6$ deposited onto ITO electrodes. The inset shows the dependence of the magnitude of the light-on photocurrent on the pH of the 0.5 M KCl electrolyte solution.

smaller than that observed with the D96N mutant (about 3 s for the light-on current and about 6 s for the light-off current), even after taking into account that these times are variable depending on the protein concentration, film thickness, and light intensity.[31] The difference between these two bR materials is that the protonable aspartate at the 96 position has been replaced by a nonprotonable asparagine in the D96N mutant. This substitution makes the decay rate of the M intermediate much slower,[33,34] because the deprotonated Schiff base cannot reprotonate from Asn96 and is forced to obtain the proton from the solution medium only. This creates a barrier for the proton uptake in the D96N mutant and makes the magnitude of the light-off peak much smaller than that of the light-on peak since the light-on photocurrent corresponds to net proton release determined by the formation of M intermediate and the light-off photocurrent relative to net proton uptake determined by the decay of M intermediate.[13,14]

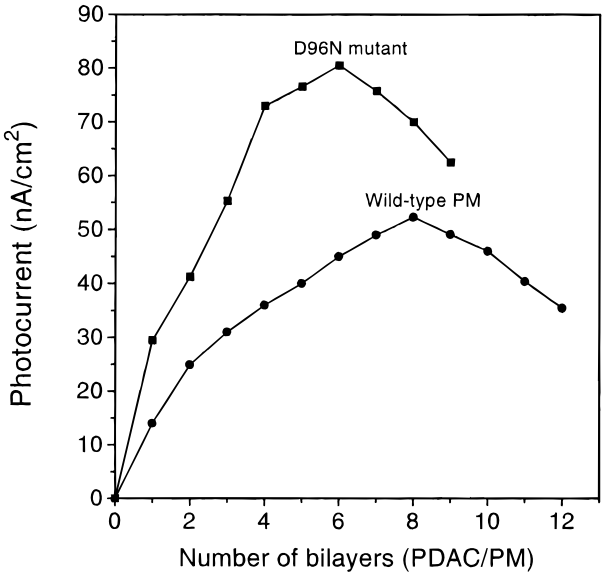

Figure 4. Magnitude of the light-on photocurrent versus the number of bilayers of PDAC/bR. The electrolyte solution is 0.5 M KCl, pH 8.5 for the WT-PM and pH 7.2 for D96N mutant.

Figure 4 shows a plot of the dependence of the light-on peak photocurrent magnitude with the number of bilayers in the PDAC/bR assemblies. Maximum values of 52 nA/cm^2 for the $(PDAC/WT\text{-}PM)_8$ and 80 nA/cm^2 for the $(PDAC/D96N)_6$ are observed. These results indicate that the photoelectric sensitivity of the D96N mutant is higher than that of the WT-PM since a larger photoelectric response is observed with the thinner D96N assembly. At this time, however, there is not sufficient evidence to conclude that this difference in photoelectric sensitivity is only due to a difference of the intrinsic quantum efficiency for proton translocation of the proteins. Another possible explanation may be due to the differing permanent electric dipole moments or surface charge densities of the WT-PM and D96N. Since the absorbance measurements in Figure 1 show that identical amounts of the WT-PM and D96N mutant are adsorbed onto the PDAC layers, the photocurrent difference may be due to inhomogeneity of the orientation of the WT-PM and D96N mutant multilayers. It has been shown that the permanent electric dipole moments or surface charge densities of the wild type and mutants of bR are quite different as a result of a single amino acid exchange in bR.[35,36] This difference could lead to varying degrees of inhomogeneity in the orientation of these multilayers during the electrostatic layer-by-layer deposition process.

From Figure 4, a peak photocurrent is also observed for both systems after only a few bilayers. As more layers are added, a decrease in photocurrent is observed which may be explained by a gradual accumulation of film resistance. This observation is also in agreement with previous conclusions stating that the contribution of the photocurrent from bR films is largely a surface effect rather than a volume effect.[13] Moreover, here the magnitude of the differential photocurrent can be strictly correlated with the exact thickness and the number of bilayers of the PDAC/bR multilayers. The optimal six (for D96N mutant) and eight (for WT-PM) bilayers are expected to be 33 and 44 nm in thickness in the PDAC/bR multilayer assemblies.[16]

3.3. Effect of Azide on the Photocurrent. To understand the mechanism of photocurrent generation of bR in these assemblies, the effect of sodium azide (NaN_3) was investigated. Figure 5 shows a plot of the magnitude of the light-on (curve 1) and light-off (curve 2) photocurrents versus concentration

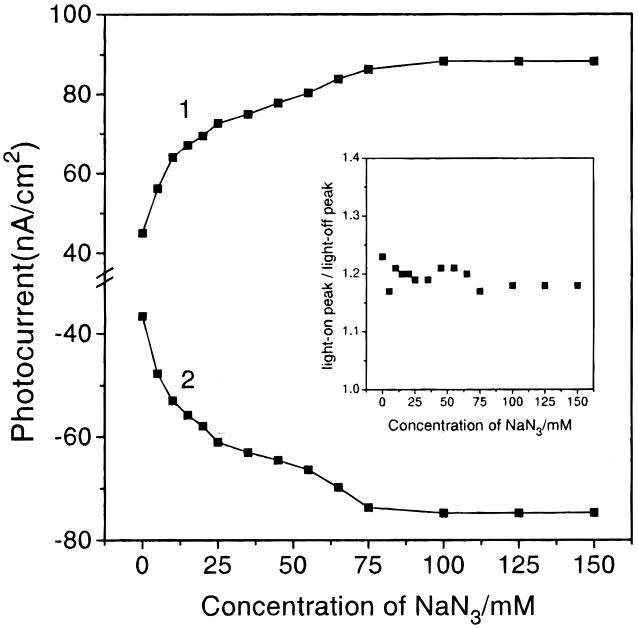

Figure 5. Magnitude of the light-on photocurrent (curve 1) and light-off photocurrent (curve 2) for a $(PDAC/WT\text{-}PM)_6$ film with concentration of NaN_3 in the 0.5 M KCl, pH 8.5 electrolyte solution. The inset shows the ratio of the magnitude of the light-on photocurrent to light-off photocurrent with the concentration of NaN_3.

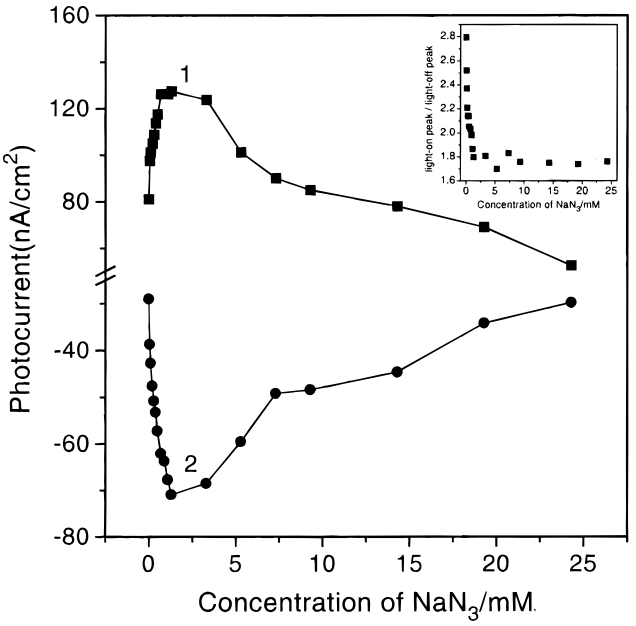

Figure 6. Magnitude of the light-on photocurrent (curve 1) and light-off photocurrent (curve 2) for a $(PDAC/D96N)_6$ film with the concentration of NaN_3 in 0.5 M KCl, pH 7.2 electrolyte solution. The inset shows the ratio of the magnitude of the light-on photocurrent to light-off photocurrent with the concentration of NaN_3.

of NaN_3 for the WT-PM; the inset is the dependence of the ratio of the magnitude of light-on to light-off peak photocurrent on the concentration of NaN_3. It is observed that the dependences of the magnitudes of the light-on and -off photocurrents with the concentration of sodium azide are divided into two stages. In the first stage the photocurrents increase with an increase in the concentration of NaN_3 below 100 mM. In the second stage the photocurrents reach a saturated value of 88 nA/cm^2 for the light-on component and -75 nA/cm^2 for the light-off current and remain unchanged from that point on with increasing concentrations of NaN_3 above 100 mM. The magnitude of the differential photocurrents roughly doubles with addition of NaN_3 to the electrolyte solution in comparison with that in the absence of NaN_3 in the electrolyte solution. The inset of Figure 5 indicates that the ratios of the light-on current to the light-off current at different concentrations of NaN_3 are a constant value of about 1.2. The results show that both the light-on photocurrent and the light-off current increase with the addition of NaN_3, and the increasing rates of these photocurrents are basically identical. Recent studies have shown that this type of increase is expected and is due to the azide's ability to catalyze the proton-transfer steps which accelerates M formation and decay by about 2 times in the WT-PM.[37] Since the M formation and decay of the bR photocycle are directly correlated with the proton release and uptake which result in the local net change of proton concentration, thus this change of proton concentration in the presence of NaN_3 with photoexcitation leads to an increase of about 2-fold of the photocurrents based on the conclusion of El-Sayed's group, which suggests that the differential current results mainly from the change in the proton concentration at the bR/ITO/electrode interface.[14] This correlation between the differential photocurrent and the concentration of NaN_3 is further evidence that the millisecond differential photocurrent originates from the local pH change, which is due to the change of proton concentration from M formation and decay. The formation of M intermediate (which leads to an increase of proton concentration at the electrode/electrolyte interface due to proton release of bR) produces the light-on photocurrent; the decay of M intermediate (which results in a decrease of proton concentration at the interface due to proton uptake of bR) contributes the light-off photocurrent.

The azide effect on the differential photocurrent of D96N mutant further verifies our above viewpoint. The dependence of the magnitude of the light-on photocurrent (curve 1) and light-off photocurrent (curve 2) on the concentration of NaN_3 for the D96N mutant is presented in Figure 6. The inset shows the change of the ratio of the magnitude (defined by the light-on photocurrent/the light-off photocurrent) with the concentration of NaN_3. These results show that the influence of NaN_3 on the photocurrent of D96N mutant is significantly different from that observed with the WT-PM. First, the magnitudes of both the light-on and light-off photocurrent increase sharply within a narrow concentration range of NaN_3 (<1.3 mM), which is in accordance with the observed azide effect on the photocurrent of the WT-PM, and show that NaN_3 can accelerate the formation and decay of M intermediate in D96N, resulting in an increasing change of proton concentration at the electrode/electrolyte interface. The increasing rate of the light-on photocurrent is the same as that of the light-off photocurrent in the presence of NaN_3 for the WT-PM (the inset of Figure 5). On the other hand, the increasing rate of the light-on photocurrent in D96N mutant is slower than that of the light-off current with concentration increase of NaN_3 presented in the inset of Figure 6. This behavior may be explained by the known ability of NaN_3 to not only catalyze proton transfer in bR but also compensate for the kinetic defect of the D96N mutant which causes a dramatic retardation of the M decay.[38,39] As shown previously in Figure 3b, the magnitude of the D96N light-off photocurrent is observed to be significantly smaller than that of the light-on photocurrent because the mutant lacks a proton donor and must make the proton uptake more slowly from the solution medium. The inset in Figure 6 illustrates the effect of this kinetic defect as a large light-on/light-off ratio is observed at very low concentrations of NaN_3. Conversely, as NaN_3 is added, the light-on/light-off ratio rapidly decreases to a constant value of approximately 1.7, showing that the NaN_3 is able to

compensate for the mutant's lack of a proton donor. This result further verifies that the light-on photocurrent comes mainly from the net proton release due to the formation of M intermediate and the light-off photocurrent originates from the net proton uptake due to the decay of M intermediate. Second, the magnitudes of both the light-on and light-off photocurrent of the D96N mutant gradually decrease as the concentration of NaN_3 is increased above 1.3 mM. For the WT-PM, no decrease of photocurrent was observed for concentrations of NaN_3 as high as 150 mM. This negative effect of azide on the photocurrent in D96N mutant is not expected and perhaps is due to the effect of catalyst poisoning.

4. Conclusion

In this work it has been demonstrated that photoelectric PDAC/bR multilayer assemblies can be successfully fabricated using alternating layer-by-layer electrostatic adsorption. The generation of photocurrent from these assemblies shows that the biological activity of the bR is preserved after deposition. This electrostatic layering technique should prove to be an effective and facile method for the fabrication of a host of bioelectronic and biooptical ultrathin devices as a variety of interesting counterions can ultimately be integrated into these assemblies to build in additional functionality. Also, the effect of NaN_3 on the differential photocurrent of WT-PM and D96N mutant supports the conclusion that the light-on photocurrent and the light-off photocurrent originate mainly from the formation and the decay of M intermediate, respectively, which in turn leads to a change in proton concentration and pH at the electrode/electrolyte interface.

Acknowledgment. Financial support from the U.S. Army NRDEC is gratefully acknowledged. Discussions with Prof. Michael Rubner at MIT, Dr. Howard H. Weetall at NIST, and Dr. Joseph Akarra at the U.S. Army NRDEC are also acknowledged. The D96N mutant in the present work is kindly provided by Dr. Weetall.

References and Notes

(1) Oesterhelt, D.; Stoeckenius, W. *Nature New Biol.* **1971**, *233*, 149.
(2) Oesterhelt, D.; Stoeckenius, W. *Proc. Natl. Acad. Sci. U.S.A.* **1973**, *70*, 2853.
(3) Lanyi, J. K. *Biochim. Biophys. Acta* **1993,** *1183*, 241.
(4) Pebay-Peyroula, E.; Rummel, G.; Rosenbusch, J. P.; Landau, E. M. *Science* **1997,** *277*, 1676.
(5) Mathies, R. A.; Lin, S. W.; Ames, J. B.; Pollard, W. T. *Annu. Rev. Biophys. Biophys. Chem.* **1991**, *20*, 491.
(6) Birge, R. R. *Annu. Rev. Phys. Chem.* **1990**, *41*, 683.
(7) Lanyi, J. K. *J. Bioenerg. Biomembr.* **1992**, *24*, 169.
(8) Cao, Y.; Brown, L. S.; Needleman, R.; Lanyi, J. K. *Biochemistry* **1993**, *32*, 10239.
(9) Zimanyi, L.; Varo, G.; Chang, M.; Ni, B.; Needleman, R.; Lanyi, J. K. *Biochemistry* **1992**, *31*, 8535.
(10) Miyasaka, T.; Koyama, K. *Appl. Opt.* **1993**, *32*, 6371.
(11) Wang, J. P.; Li, J. R.; Tao, P. D.; Li, X. C.; Jiang, L. *Adv. Mater. Opt. Electron.* **1994,** *4*, 219.
(12) (a) Miyasaka, T.; Koyama, K.; Otoh, I. *Science* **1992**, *255*, 342. (b) Koyama, K.; Yamaguchi, N.; Miyasaka, T. *Adv. Mater.* **1995**, *7*, 590.
(13) Robertson, B.; Lukashev, E. P. *Biophys. J.* **1995**, *68*, 1507.
(14) (a) Wang, J. P.; Yoo, S. K.; Song, L.; El-Sayed, M. A. *J. Phys. Chem. B* **1997**, *101*, 3420. (b) Wang, J. P.; Song, L.; Yoo, S. K.; El-Sayed, M. A. *J. Phys. Chem. B* **1997**, *101*, 10599.
(15) (a) Decher, G. *Science* **1997**, *277*, 1232. (b) Ferreira, M.; Cheung, J. H.; Rubner, M. F. *Thin Solid Films* **1994**, *244*, 806.
(16) He, J. A.; Samuelson, L.; Li, L.; Kumar, J.; Tripathy, S. K. *Langmuir* **1998,** *14*, 1674.
(17) Bouevitch, O.; Lewis, A. *Opt. Commun.* **1995**, *116*, 170.
(18) Oesterhelt, D.; Stoeckenius, W. *Methods Enzymol.* **1974**, *31*, 667.
(19) Oesterhelt, D. *Nature* **1989**, *338*, 16.
(20) Gergely, C.; Zimanyi, L.; Varo, G. *J. Phys. Chem. B* **1997,** *101*, 9390.
(21) Jonas, R.; Koutalos, Y.; Ebrey, T. G. *Photochem. Photobiol.* **1990**, *52*, 1163.
(22) Ehrenberg, B.; Ebrey, T. G.; Friedman, N.; Sheves, M. *FEBS Lett.* **1989,** *250*, 179.
(23) Alexiev, U.; Marti, T.; Heyn, M. P.; Khorana, H. G.; Scherer, P. *Biochemistry* **1994,** *33*, 298.
(24) Ikonen, M.; Peltonen, J.; Vuorimaa, E.; Lemmetyinen, H. *Thin Solid Films* **1992**, *213*, 277.
(25) Keszthelyi, L. *Biochim. Biophys. Acta* **1980**, *598*, 429.
(26) Koyama, K.; Yamaguchi, N.; Miyasaka, T. *Science* **1994**, *265*, 762.
(27) Ferreira, M.; Rubner, M. F. *Macromolecules* **1995**, *28*, 7107.
(28) (a) Lvov, Y.; Ariga, K.; Onda, M.; Ichinose, I.; Kunitake, T. *Langmuir* **1997**, *13*, 6195. (b) Fendler, J. H. *Chem. Mater.* **1996,** *8*, 1616.
(29) Lvov, Y.; Ariga, K.; Ichinose, I.; Kunitake, T. *J. Am. Chem. Soc.* **1995**, *117*, 6117.
(30) (a) Sun, Y. P.; Hao, E. C.; Zhang, X.; et al. *Langmuir* **1997**, *13*, 5168. (b) Lvov, Y.; Ariga, K.; Ichinose, I.; Kunitake, T. *Langmuir* **1996**, *12*, 3038.
(31) Chen, Z. P.; Birge, R. R. *TIBTECH* **1993**, *11*, 292.
(32) Lu, T.; Li, B. F.; Jiang, L.; Rothe, U.; Bakowsky, U. *J. Chem. Soc., Faraday Trans.* **1998**, *94*, 79.
(33) Butt, H. J.; Fendler, K.; Bamberg, E.; Tittor, J.; Oesterhelt, D. *EMBO J.* **1989**, *8*, 1657.
(34) Miller, A.; Oesterhelt, D. *Biochim. Biophys. Acta* **1990,** *1020*, 57.
(35) Hsu, K. C.; Rayfield, G. W.; Needleman, R. *Biophys. J.* **1996**, *70*, 2358.
(36) Mostafa, H. I. A.; Varo, G.; Toth-Boconadi, R.; Keszthelyi, L. *Biophys. J.* **1996**, *70*, 468.
(37) LeCoutre, J.; Tittor, J.; Oesterhelt, D.; Gerwert, K. *Proc. Natl. Acad. Sci. U.S.A.* **1995**, *92*, 4962.
(38) Drachev, L. A.; Kaulen, A. D.; Komrakov, A. Y. *FEBS Lett.* **1992,** *313*, 248.
(39) Tittor, J.; Soell, C.; Oesterhelt, D.; Butt, H. J.; Bamberg, E. *EMBO J.* **1989**, *8*, 3477.